Effects of cochlear loading on the motility of active outer hair cells

Supporting Information Appendix

Dáibhid Ó Maoiléidigh and A. J. Hudspeth

Howard Hughes Medical Institute and Laboratory of Sensory Neuroscience

The Rockefeller University, New York, NY 10065-6399, USA

1 Active Hair-Bundle Mechanics

In the absence of stimulation a "silent current" flows through an active OHC [1]. We define this configuration for a fixed set of parameters to be the reference state. All the equations of motion for the OHC represent expansions around this state.

In the cochlea the hair bundle of an OHC is directly loaded by the mass $m_{\rm tm}$ of the tectorial membrane, the effective damping $\lambda_{\rm tm}$ of the tectorial membrane, reticular lamina, and fluid between these structures, and the effective stiffness $K_{\rm tm}$ of the tectorial membrane and reticular lamina. Feedback from somatic motility can result in a reduction in the effective damping of the bundle [2], which is taken into account by specifying a negative value for $\lambda_{\rm tm}$. An active, loaded hair bundle is described by

$$\begin{aligned} m_{\rm tm}\ddot{X}_{\rm hb} = &-(\lambda_{\rm hb}+\lambda_{\rm tm})\dot{X}_{\rm hb} - K_{\rm gs}(X_{\rm hb}-X_{\rm a}-X_{\rm gs}-DP_{\rm o}) \\ &- (K_{\rm sp}+K_{\rm tm})(X_{\rm hb}-X_{\rm sp}) + F_{\rm hb} \end{aligned} \tag{S1}$$

$$\lambda_{\rm a}\dot{X}_{\rm a} = K_{\rm gs}(X_{\rm hb}-X_{\rm a}-X_{\rm gs}-DP_{\rm o}) - K_{\rm a}(1-\alpha P_{\rm o})(X_{\rm a}-X_{\rm r}) \tag{S2}$$

$$P_{\rm o} = \frac{1}{1+Ae^{-(X_{\rm hb}-X_{\rm a})/\delta}}, \tag{S3}$$

in which $X_{\rm hb}$ and $X_{\rm a}$ are respectively the displacement of the hair bundle and the extension of the adaptation springs and $F_{\rm hb}$ is the external force on the bundle (Fig. 1B). The gating springs are parameterized by their effective stiffness $K_{\rm gs}$, reference extension $X_{\rm gs}$, and gating swing D [3]. The reference extension of the stereociliary-pivot springs, which underlie the bundle's linear stiffness $K_{\rm sp}$, is denoted by $X_{\rm sp}$. The damping coefficient of the hair bundle is $\lambda_{\rm hb}$. The open probability $P_{\rm o}$ of the mechanoelectrical-transduction channels is a nonlinear function of $X_{\rm hb}$ and $X_{\rm a}$ in which $1/(1+A)$ is the probability when the gating springs are cut and δ is the length scale for channel opening. Both A and δ depend upon the number N of transduction channels, the energy ΔG for chan-

nel opening, a geometric factor γ, the Boltzmann constant k_B, and the temperature T as $A = \exp\left[\Delta G + K_\mathrm{gs} D^2/(2Nk_\mathrm{B}T) + K_\mathrm{gs} D X_\mathrm{gs}/(\gamma N k_\mathrm{B} T)\right]$ and $\delta = Nk_\mathrm{B}T/(K_\mathrm{gs} D)$ [3, 4]. All the relevant variables and parameters refer to measurements made at the hair bundle's top along its axis of maximal sensitivity.

The activity of the hair bundle results from the dynamics of the adaptation springs with damping λ_a, reference extension X_r, and maximal stiffness K_a. The stiffness of the adaptation springs declines upon Ca^{2+} binding with a sensitivity α, in which $0 \leq \alpha \leq 1$. As is evident from their distinct mathematical formulations, this adaptation mechanism differs from a previous proposal that made the gating-spring stiffness Ca^{2+}-dependent [3, 5, 6]. The essential difference is that the gating spring's stiffness constrains the difference between hair-bundle displacement and adaptation-spring extension, whereas the adaptation spring's stiffness and viscosity constrain the extension of the adaptation spring itself.

2 Hair-Bundle Activity

The change in the local intracellular Ca^{2+} concentration C is described by

$$\dot{C} = -JP_\mathrm{o}V_\mathrm{ohc} - J(P_\mathrm{o} - P_\mathrm{o}^\mathrm{ref})(V_\mathrm{ohc}^\mathrm{ref} - V_\mathrm{sm} - E_\mathrm{Ca}) - \rho C, \tag{S4}$$

in which V_ohc is the receptor potential, $P_\mathrm{o}^\mathrm{ref}$ is the reference open probability of the transduction channels, $V_\mathrm{ohc}^\mathrm{ref}$ is the resting potential, V_sm is the potential of the scala media, $E_\mathrm{Ca} \approx 0$ is the reversal potential for Ca^{2+}, and ρ is the rate constant for removal of free Ca^{2+} by pumps and buffers. The parameter $J = g_\mathrm{Ca}^\mathrm{max}/(2ewN_\mathrm{A})$, in which $g_\mathrm{Ca}^\mathrm{max}$ is the hair bundle's maximal Ca^{2+} conductance, e is the charge of the electron, w is an effective volume, and N_A is Avogadro's number. The formulation of the adaptation-spring model (Eqs. S1-S3) assumes that the intrinsic Ca^{2+} dynamics is sufficiently fast that $\dot{C} \approx 0$. A further simplification can be

made by noting that $|(P_\mathrm{o} - P_\mathrm{o}^\mathrm{ref})(V_\mathrm{ohc}^\mathrm{ref} - V_\mathrm{sm} - E_\mathrm{Ca})| \gg |P_\mathrm{o} V_\mathrm{ohc}|$, for $|V_\mathrm{ohc}^\mathrm{ref} - V_\mathrm{sm}| \gg |V_\mathrm{ohc}|$. These two approximations yield $C = -J(P_\mathrm{o} - P_\mathrm{o}^\mathrm{ref})(V_\mathrm{ohc}^\mathrm{ref} - V_\mathrm{sm} - E_\mathrm{Ca})/\rho$. The adaptation spring's stiffness is then given to linear order in the Ca^{2+} concentration by

$$\kappa_\mathrm{a} = \kappa_\mathrm{a}^\mathrm{ref} + \kappa_\mathrm{a}' C = K_\mathrm{a}(1 - \alpha P_\mathrm{o}), \tag{S5}$$

in which $\kappa_\mathrm{a}^\mathrm{ref}$ is the stiffness of the adaptation spring in the reference state, $\kappa_\mathrm{a}' < 0$ is the derivative of the stiffness with respect to the Ca^{2+} concentration in the reference state, $K_\mathrm{a} = \kappa_\mathrm{a}^\mathrm{ref} + \kappa_\mathrm{a}' J P_\mathrm{o}^\mathrm{ref}(V_\mathrm{ohc}^\mathrm{ref} - V_\mathrm{sm} - E_\mathrm{Ca})/\rho$, and $\alpha = (1 - \kappa_\mathrm{a}^\mathrm{ref}/K_\mathrm{a})/P_\mathrm{o}^\mathrm{ref}$. Thus K_a and α both depend upon the processes that maintain the OHC's resting potential $V_\mathrm{ohc}^\mathrm{ref}$ and the endocochlear potential $V_\mathrm{sm} - V_\mathrm{st} \approx V_\mathrm{sm}$, the Ca^{2+} reversal potential E_Ca, and Ca^{2+} pumps that contribute to the rate ρ. In a passive system $V_\mathrm{ohc}^\mathrm{ref} = 0$ and $V_\mathrm{sm} = 0$ such that $K_\mathrm{a} \approx \kappa_\mathrm{a}^\mathrm{ref}$ and $\alpha \approx 0$.

3 Transduction-Channel Sensitivity

The sensitivity of the mechanosensitive channel's open probability P_o to hair-bundle deflection is determined by its characteristic width δ (Eq. S3). The channel's open probability P_o can be found experimentally by measuring the current through the bundle relative to the maximal value [7, 8]. One method for calculating δ is to measure the peak responses of the hair bundle to step forces of various magnitudes [7]. Applying this analysis to numerical simulations of hair-bundle responses to step stimuli (Fig. 1C) we obtain the value $\delta_\mathrm{app} = 30.3 \pm 0.9$ nm (Fig. S1A), which accords with a recent experimental measurement of $\delta_\mathrm{expt} = 35$ nm [8]. The apparent value for δ, however, is severalfold the value of δ actually used in simulations, $\delta = 4.2$ nm. This disparity arises because P_o depends upon the adaptation process that recloses the channels during the period of stimulation. Our analy-

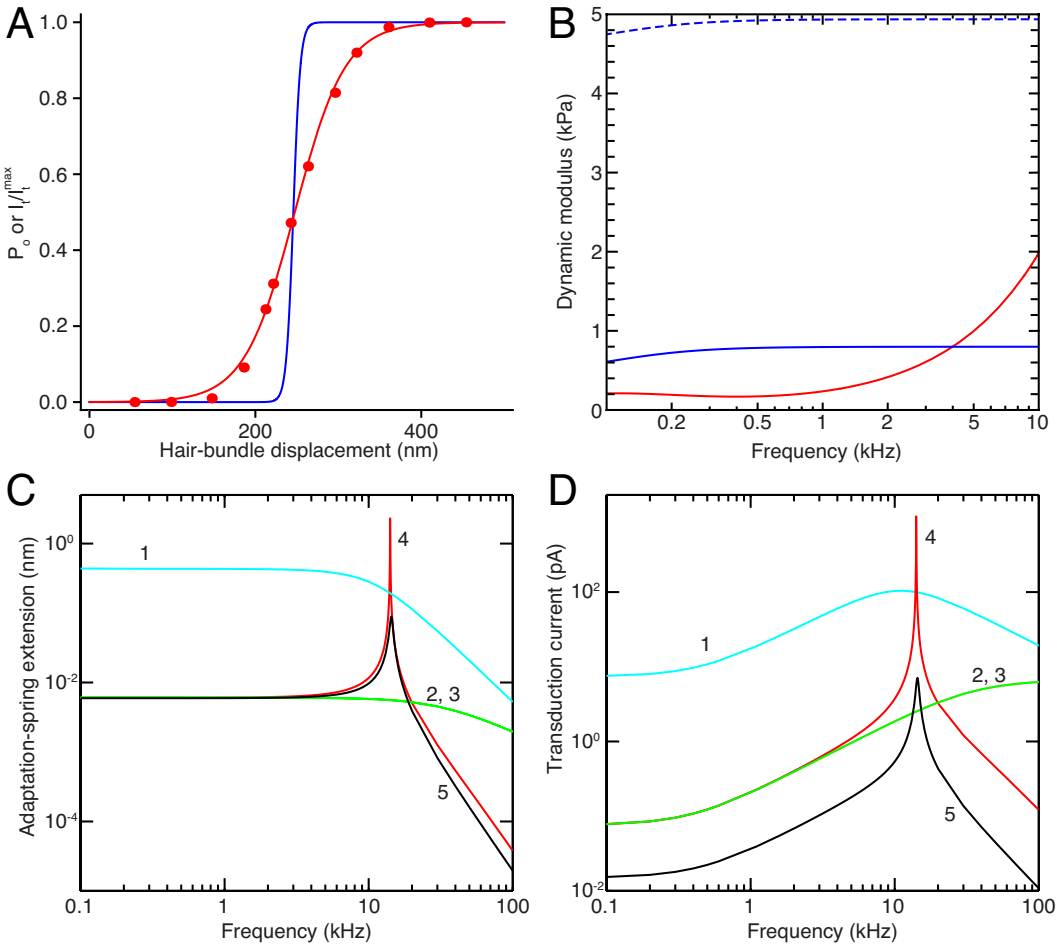

Figure S1: (A) The open probability P_o of mechanoelectrical-transduction channels (Eq. S3) is shown as a function of bundle displacement for $X_\mathrm{a} = 220$ nm (blue line). The normalized magnitude of the transduction current $I_\mathrm{t}/I_\mathrm{t}^\mathrm{max}$ in response to step stimulation (Fig. 1C and four other determinations) is plotted against bundle displacement (red dots). These data are fit to Eq. S3 with X_a fixed (red line) and yield $\delta_\mathrm{app} = 30.3\pm0.9$ nm ($R^2 = 1.00$, p-value $< 10^{-11}$). (B) The real part (solid blue line) and imaginary part (solid red line) of the OHC's dynamic modulus after treatment with 9AC are portrayed as a function of the stimulus frequency. The real part of the dynamic modulus changes when somatic motility is restored (dashed blue line) whereas the imaginary part remains constant. (C) The extension of the adaptation spring is shown as a function of the stimulus frequency for different conditions (Table S1): (1) an active, unloaded OHC; (2) an active OHC with its soma loaded by the basilar-membrane stiffness K_bm and damping λ_bm, its hair bundle loaded by the effective stiffness K_tm of the tectorial membrane and basilar membrane, and a negative damping coefficient λ_tm to capture the effect of somatic feedback; (3) a similar configuration after addition of the basilar-membrane mass m_bm; (4) a similar configuration including the tectorial-membrane mass m_tm; and (5) after removal of hair-bundle activity by reduction of K_a and α. (D) The transduction current is shown as a function of the stimulus frequency for the same five conditions.

sis suggests that the nonlinearity of transduction has been significantly underestimated by contemporary experimental techniques owing to the speed of the adaptation process. The single-channel gating force $Z = k_{\mathrm{B}}T/\delta$ has therefore been underestimated by more than an order of magnitude [9–11]. We find that the gating force increases from $Z = 10$ pN at 4 kHz to $Z = 19$ pN at 14 kHz primarily owing to the decrease in the hair bundle's length (Sections 1 and 8).

4 Resonant Frequency of the Loaded Hair Bundle

The resonant frequency f_{r} of a loaded hair bundle depends on the properties of the bundle in a complex fashion and also exhibits a nonlinear dependence on the amplitude of external forcing. If we consider the response in the limit of zero forcing and the operating point of the hair bundle is at a supercritical Hopf bifurcation, however, it is possible to find an expression for f_{r} with a simpler parameter dependence.

There is a real, steady-state solution to Eqs. S1 and S2 in the absence of forcing ($F_{\mathrm{hb}} = 0$) at a supercritical Hopf bifurcation. To linear order near this solution Eqs. S1 and S2 may be written as

$$\begin{pmatrix} \dot{X}_{\mathrm{hb}} \\ \dot{V}_{\mathrm{hb}} \\ \dot{X}_{\mathrm{a}} \end{pmatrix} = \begin{pmatrix} 0 & 1 & 0 \\ -(K_{\mathrm{GS}} + K_{\mathrm{sp}} + K_{\mathrm{tm}})/m_{\mathrm{tm}} & -(\lambda_{\mathrm{hb}} + \lambda_{\mathrm{tm}})/m_{\mathrm{tm}} & K_{\mathrm{GS}}/m_{\mathrm{tm}} \\ (K_{\mathrm{GS}} + K_{\mathrm{A}})/\lambda_{\mathrm{a}} & 0 & -K_{\mathrm{a,eff}}/\lambda_{\mathrm{a}} \end{pmatrix} \begin{pmatrix} X_{\mathrm{hb}} \\ V_{\mathrm{hb}} \\ X_{\mathrm{a}} \end{pmatrix}, \quad \text{(S6)}$$

in which $V_{\mathrm{hb}} = \dot{X}_{\mathrm{hb}}$ is the hair bundle's velocity, $K_{\mathrm{GS}} = K_{\mathrm{gs}}(1 - DP_{\mathrm{o}}')$, $K_{\mathrm{A}} = K_{\mathrm{a}}\alpha P_{\mathrm{o}}'(X_{\mathrm{a}}^{\star} - X_{\mathrm{r}})$, $K_{\mathrm{a,eff}} = K_{\mathrm{GS}} + K_{\mathrm{A}} + K_{\mathrm{a}}(1 - \alpha P_{\mathrm{o}}^{\star})$, $P_{\mathrm{o}}' = \partial_X P_{\mathrm{o}}(X)^{\star}$, and the asterisk signifies that an expression is to be evaluated at the steady-state solution. The eigenvalues μ of the matrix satisfy the

characteristic equation

$$0 = a\mu^3 + b\mu^2 + c\mu + d, \tag{S7}$$

in which

$$a = \frac{m_{\mathrm{tm}}}{\lambda_{\mathrm{hb}} + \lambda_{\mathrm{tm}}} \tag{S8}$$

$$b = 1 + \frac{m_{\mathrm{tm}}}{\lambda_{\mathrm{hb}} + \lambda_{\mathrm{tm}}} \left(\frac{K_{\mathrm{a,eff}}}{\lambda_{\mathrm{a}}} \right) \tag{S9}$$

$$c = \frac{K_{\mathrm{a,eff}}}{\lambda_{\mathrm{a}}} + \frac{K_{\mathrm{GS}} + K_{\mathrm{sp}} + K_{\mathrm{tm}}}{\lambda_{\mathrm{hb}} + \lambda_{\mathrm{tm}}} \tag{S10}$$

$$d = \left(\frac{K_{\mathrm{a,eff}}}{\lambda_{\mathrm{a}}} \right) \left(\frac{K_{\mathrm{GS}} + K_{\mathrm{sp}} + K_{\mathrm{tm}}}{\lambda_{\mathrm{hb}} + \lambda_{\mathrm{tm}}} \right) - \left(\frac{K_{\mathrm{GS}}}{\lambda_{\mathrm{hb}} + \lambda_{\mathrm{tm}}} \right) \left(\frac{K_{\mathrm{GS}} + K_{\mathrm{A}}}{\lambda_{\mathrm{a}}} \right). \tag{S11}$$

A Hopf bifurcation is defined to occur when an eigenvalue of the system is imaginary and can therefore be written as $\mu = i2\pi f_{\mathrm{r}}$. Substituting this expression into Eqs. S8-S11 yields

$$f_{\mathrm{r}} = \frac{1}{2\pi} \sqrt{\frac{d}{b}} = \frac{K_{\mathrm{eff}}}{\sqrt{(\lambda_{\mathrm{hb}} + \lambda_{\mathrm{tm}})\lambda_{\mathrm{a}} + m_{\mathrm{tm}} K_{\mathrm{a,eff}}}}, \tag{S12}$$

in which $K_{\mathrm{eff}} = \sqrt{(K_{\mathrm{GS}} + K_{\mathrm{sp}} + K_{\mathrm{tm}})K_{\mathrm{a,eff}} - (K_{\mathrm{GS}} + K_{\mathrm{A}})K_{\mathrm{GS}}}/(2\pi)$. Even though this equation has been derived for an unstimulated hair bundle operating at a Hopf bifurcation, it is approximately correct for a quiescent bundle operating near such a bifurcation for weak forcing [12].

5 Somatic Electromechanics

In most experiments on isolated OHCs the membrane potential and force on an OHC are controlled and the resulting axial extension or charge displacement across the basolateral membrane of the cell is measured [13, 14]. The extension of an OHC is weakly nonlinear

within the physiological range of the membrane potential of ±20 mV [8] around the reference potential of −35 mV [13]. To a good approximation within this range, the steady-state charge displacement across the OHC's basolateral membrane $Q(F,V)$ and the steady-state OHC extension $X(F,V)$ are given in terms of their linear response to changes in the axial force applied to the OHC F and the basolateral membrane potential V as

$$Q - Q_{\text{ref}} = \left.\frac{\partial Q}{\partial F}\right|_{\text{ref}} (F - F_{\text{ref}}) + \left.\frac{\partial Q}{\partial V}\right|_{\text{ref}} (V - V_{\text{ref}}) \tag{S13}$$

$$X - X_{\text{ref}} = \left.\frac{\partial X}{\partial F}\right|_{\text{ref}} (F - F_{\text{ref}}) + \left.\frac{\partial X}{\partial V}\right|_{\text{ref}} (V - V_{\text{ref}}) \,, \tag{S14}$$

in which the subscript ref indicates that the expression is to be evaluated at the reference state. These equations may be rewritten as

$$q = eF_{\text{s}} + CV_{\text{ohc}} \tag{S15}$$

$$X_{\text{ohc}} = K^{-1}F_{\text{s}} + eV_{\text{ohc}}, \tag{S16}$$

in which the capacitance C, stiffness K, and negative piezoelectric coefficient e depend on the reference state and have been measured experimentally. In particular, the capacitance C depends on the reference membrane potential. This voltage dependence over very large changes in membrane potential has been termed nonlinear capacitance and has been used to indicate the presence of somatic motility in many experiments [13, 14]. In other words, C is not constant for large changes in the reference potential and can be greatly increased by the presence of somatic motility [14]. The value for this capacitance used here (14 pF) is accordingly more than twice [14] the linear capacitance of a 14 kHz cell at −35 mV (5 pF) [8] and is about twice the value owing solely to the geometry of the basolateral wall of the 25 μm OHC (8 pF).

In the cochlea, the membrane potential and the force applied on an OHC result from

charge displacement arising from the changing conductance of the transduction channel and from contact with surrounding cochlear structures, rather than being inputs to each OHC. Equations S15 and S16 may be rearranged to yield

$$F_{\mathrm{s}} = \left(\frac{C}{CK^{-1} - e^2}\right) X_{\mathrm{ohc}} - \left(\frac{e}{CK^{-1} - e^2}\right) q \tag{S17}$$

$$V_{\mathrm{ohc}} = -\left(\frac{e}{CK^{-1} - e^2}\right) X_{\mathrm{ohc}} + \left(\frac{K^{-1}}{CK^{-1} - e^2}\right) q, \tag{S18}$$

which may be rewritten as

$$F_{\mathrm{s}} = K_{\mathrm{p}} X_{\mathrm{ohc}} + pq \tag{S19}$$

$$V_{\mathrm{ohc}} = pX_{\mathrm{ohc}} + C_{\mathrm{b}}^{-1} q. \tag{S20}$$

This formulation for somatic motility is used in this paper. When $CK^{-1} \gg e^2$, $K_{\mathrm{p}} \approx K$, $C_{\mathrm{b}} \approx C$, and $p \approx -eK/C$. The values $C = 14$ pF [8,14], $K = 10$ mN·m^{-1} [14], and $e = -20$ μm·V^{-1} [13] determine the values for C_{b}, K_{p}, and p listed in Table S1.

For a complete description of somatic dynamics, the full mechanical impedance of an OHC, the electrodynamics of the cell, and the load afforded by the basilar membrane must be taken into account. The equations of motion corresponding to the loaded soma of an OHC (Figs. 1 and 2A, C) are

$$\dot{q}(1 + C_{\mathrm{a}}/C_{\mathrm{b}}) = -C_{\mathrm{a}} p \dot{X}_{\mathrm{ohc}} - q(g_{\mathrm{t}}^{\max} P_{\mathrm{o}}^{\mathrm{ref}} + g_{\mathrm{b}})/C_{\mathrm{b}} - pX_{\mathrm{ohc}}(g_{\mathrm{t}}^{\max} P_{\mathrm{o}}^{\mathrm{ref}} + g_{\mathrm{b}}) + I_{\mathrm{t}} \tag{S21}$$

$$\begin{aligned} m_{\mathrm{bm}} \ddot{X}_{\mathrm{ohc}} = {} & -K_{\mathrm{c}}(X_{\mathrm{ohc}} - X_{\mathrm{c}}) - (K_{\mathrm{p}} + K_{\mathrm{bm}}) X_{\mathrm{ohc}} - pq \\ & - \lambda_{\mathrm{c2}}(\dot{X}_{\mathrm{ohc}} - \dot{X}_{\mathrm{c}}) - \lambda_{\mathrm{bm}} \dot{X}_{\mathrm{ohc}} + F_{\mathrm{s}} \end{aligned} \tag{S22}$$

$$\lambda_{\mathrm{c1}} \dot{X}_{\mathrm{c}} = \lambda_{\mathrm{c2}}(\dot{X}_{\mathrm{ohc}} - \dot{X}_{\mathrm{c}}) + K_{\mathrm{c}}(X_{\mathrm{ohc}} - X_{\mathrm{c}}) \tag{S23}$$

$$V_{\mathrm{ohc}} = \frac{q}{C_{\mathrm{b}}} + pX_{\mathrm{ohc}}, \tag{S24}$$

in which X_{c} is the extension of the dashpot λ_{c1} (Fig. 2A), X_{ohc} is the change in the OHC length, q is the change in the charge on the somatic membrane, and V_{ohc} is the receptor potential. The two external forces on the system are the current I_{t} through the transduction channels and the mechanical force F_{s} on the soma. All the other parameters are defined in Figs. 1A and 2A, C. This formulation utilizes the approximation that V_{sm} and V_{st} are constant such that the changes in the potentials across the apical and basolateral membranes of the OHC are the same.

The axial mechanical impedance of an unloaded OHC treated with 9AC is given by $Z_{\mathrm{ohc}}(f) = \tilde{F}_{\mathrm{s}}(f)/\tilde{v}_{\mathrm{ohc}}(f)$, in which the tildes denote the Fourier transform, f is the forcing frequency, and the velocity $v_{\mathrm{ohc}} \equiv \dot{X}_{\mathrm{ohc}}$. The impedance of the model OHC is computed from Eqs. S22–S23 by setting $m_{\mathrm{bm}} = 0$, $K_{\mathrm{bm}} = 0$, $\lambda_{\mathrm{bm}} = 0$, $p = 0$, and $K_{\mathrm{p}} = K_{\mathrm{c}}$.

6 Dynamic Modulus

The axial dynamic modulus $G(f)$ of the cylindrical OHC is given by

$$G(f) = 2\pi \mathrm{i} f Z_{\mathrm{ohc}}(f) X_{\mathrm{ohc}}^{ref}/A_{\mathrm{ohc}}, \tag{S25}$$

in which X_{ohc}^{ref} is the reference length and A_{ohc} is the reference cross-sectional area of the OHC. The dynamic modulus of a 14 kHz OHC is calculated for $X_{\mathrm{ohc}}^{ref} = 25\,\mu$m and $A_{\mathrm{ohc}} = 25\pi\,\mu\mathrm{m}^2$ [8, 15].

7 Somatic Responses to Electrical Stimulation

The response of the OHC's soma to sinusoidal changes in the hair bundle's conductance is found from Eqs. S21–S24 with $I_{\mathrm{t}} = (V_{\mathrm{sm}} - V_{\mathrm{ohc}}^{\mathrm{ref}})(g_{\mathrm{t}}^{max}/2)\cos(2\pi f t)$, in which g_{t}^{max} is the maximal conductance of the transduction channels.

8 Hair-Bundle Scaling

Hair-bundle motility is expected to change between the 4 kHz and 14 kHz places because the bundle length L decreases from 2.9 μm to 1.6 μm [16] and the maximal transduction conductance increases from 40 nS to 75 nS [8]. The change in length affects hair-bundle mechanics significantly: $K_{\mathrm{sp}} \sim L^{-2}$, $K_{\mathrm{gs}} \sim L^{-2}$, $D \sim L$, $\lambda_{\mathrm{hb}} \sim L^{-1}$ and $\gamma \sim L^{-1}$. The rise in conductance increases the values of both K_{a} and α, for the adaptation spring becomes more sensitive to changes in the open probability (Section 2). These considerations inform the choices of the parameter values at the 14 kHz place (Table S1).

9 Coupling Active Hair-Bundle Motility and Somatic Motility

To disentangle the various contributions to the cochlear amplifier we hold the cell's apical surface in a fixed position, thereby preventing somatic motility and basilar-membrane motion from influencing the hair bundle. We subsequently reintroduce the key effects of the normal coupling by forcing the bundle to mimic its response to basilar-membrane motion in the actual cochlea. We render the effective damping of the tectorial membrane negative to reflect the effect of somatic feedback on the bundle [2] and increase the stiffness of the tectorial membrane to include the bundle's coupling to the basilar membrane by the organ of Corti. We align the resonances of the hair bundle and tectorial membrane with that of the OHC and basilar membrane. When the OHC's apex can move, however, at least two modes of vibration are possible with resonant frequencies depending upon the properties of the entire cochlear partition [17–19].

The hair bundle of an OHC and the cell's soma are linked by the transduction current $I_{\mathrm{t}} = (V_{\mathrm{sm}} - V_{\mathrm{ohc}}^{\mathrm{ref}}) g_{\mathrm{t}}^{\mathrm{max}} (P_{\mathrm{o}} - P_{\mathrm{o}}^{\mathrm{ref}})$ such that an active OHC is described by Eqs S1–S3 and S21–

S24. The response of the system to sinusoidal forcing of the bundle $F_{\rm hb} = F_{\rm hb}^{\rm max}\cos(2\pi ft)$ in the absence of somatic forcing ($F_{\rm s} = 0$) is shown in Fig. 3.

The transduction current, which depends upon the difference $X_{\rm hb} - X_{\rm a}$ (Eq. S3), is shown in Fig. S1D under the same conditions considered in Fig. 3. The current of an isolated OHC displays a maximum at 11.1 kHz because $X_{\rm hb} - X_{\rm a}$ attains a maximum even though both $X_{\rm hb}$ and $X_{\rm a}$ are low-pass filtered (Figs. 3B and S1C). As a consequence of the low-pass filtering of the receptor potential by the OHC's membrane, there is a maximum in the receptor potential and thus in the OHC's extension at a lower frequency of about 5.1 kHz (Fig. 3C, D). The effect persists when the load's stiffness and damping are introduced, but is overwhelmed by the influence of cochlear inertia.

Hair-bundle activity amplifies the transduction current at the active 14.1 kHz resonance by a factor of 186 in comparison with the passive response (Fig. S1D). This enhancement leads to amplification of the receptor potential and thus the OHC's extension by the same factor (Fig. 3C, D).

10 Parameter Values

A list of parameter values is given in Table S1. The methodology for estimating most parameter values from experimental measurements has been described previously [2]. Here we clarify some additional points.

Most parameter values required for a complete model of cochlear mechanics are not known for one species or at more than a few places along the cochlear partition. This presents a major challenge in creating models of cochlear mechanics. Detailed global models that include wave mechanics must include many assumptions about how parameter values change from one cochlear position to another [28,29], leading to a lack of consensus as to how the cochlea functions *in vivo*. To avoid this difficulty, we elect to focus on the two cochlear

locations for which most parameter values are known.

Although all of the parameter values are constrained by experimental measurements, there is some flexibility with regard to the exact values. For example, we choose values to create resonant responses very close to 4 kHz and 14 kHz. Other possible choices would produce resonances at the same frequencies or nearby frequencies. A systematic search through all possible parameter combinations, however, is beyond the scope of this work.

There are two reasons why the tectorial and basilar membranes act as mass loads on an OHC even though they have densities similar to that of the cochlear fluid. First, because the membranes are cohesive structures, they do not flow with the fluid. They are not accelerated in the same fashion as the fluid by an OHC and therefore they load an OHC differently. For example, the fluid can flow around an OHC, but the membranes cannot. Second, the other material properties of these membranes, such as their elastic and viscous moduli, are different from those of the fluid; furthermore, the membranes are attached to the cochlear bone. The model must therefore treat the membranes differently than the fluid.

We estimate the total mass of the tectorial and basilar membranes as the products of their volumes and densities. Each membrane is a spatially distributed object, however, that may not move as a unit with an OHC. The effective mass loads of an OHC may thus be less than the membranes' total mass. For example, in the gerbil the tectorial-membrane volume for a cochlear segment one OHC diameter wide is $3.5 \times 10^4 \mu\text{m}^3$ [27,30] near the 14 kHz place, yielding a total mass of 35 ng. We use a value of 26 ng in the model.

Bundle motility		4 kHz	Ref.	14 kHz	Ref.	Somatic motility		14 kHz	Ref.
X_{sp}	nm	285	20	285	20	λ_{c1}	μN·s·m^{-1}	1.99	Fit B
X_{r}	nm	-285	Fit A	-285	Fit A	λ_{c2}	nN·s·m^{-1}	104	Fit B
λ_{a}	nN·s·m^{-1}	140	Fit A	140	Fit A	K_{c}	mN·m^{-1}	1.32	Fit B
λ_{hb}	nN·s·m^{-1}	150	16, 21	100	16, 21	$K_{\mathrm{p}}^{\mathrm{9AC}}$	mN·m^{-1}	1.32	Fit B
ΔG	k_{B}T	10	3	10	3	K_{p}	mN·m^{-1}	14.3	14
T	K	300	3	310	8	p	kV·m^{-1}	20	22
X_{gs}	nm	-7.1	3	-8	3	C_{b}	pF	10	8
N	—	110	23	116	23	C_{a}	pF	$C_{\mathrm{b}}/5$	8
D	nm	24	3, 9	14	Scale	g_{b}	nS	285	8
K_{gs}	mN·m^{-1}	4.5	7	16	Scale	$g_{\mathrm{t}}^{\mathrm{ref}}$	nS	75	8
K_{sp}	mN·m^{-1}	1	7	3	Scale	$P_{\mathrm{o}}^{\mathrm{ref}}$	—	0.5	8
γ	—	0.25	9	0.44	Scale	$V_{\mathrm{ohc}}^{\mathrm{ref}}$	mV	-35	8
δ	nm	4.22	Calc.	2.22	Calc.	V_{sm}	mV	85	24
A	—	451	Calc.	143	Calc.	V_{st}	mV	0	24
						E_{t}	mV	0	23

Bundle load		4 kHz	Ref.	14 kHz	Ref.	Somatic load		14 kHz	Ref.
K_{tm}	mN·m^{-1}	20	25, 26	203	25, 26	K_{bm}	mN·m^{-1}	300	26
λ_{tm}	nN·s·m^{-1}	-124		-60		λ_{bm}	nN·s·m^{-1}	104	
m_{tm}	ng	32	27	26	27	m_{bm}	ng	40	27
K_{f}	mN·m^{-1}	2	7						
λ_{f}	nN·s·m^{-1}	350	7						

Bundle activity		4 kHz	Ref.	4 kHz	Ref.	14 kHz	Ref.	14 kHz	Ref.
K_{a}	μN·m^{-1}	400	Fit A	400	Pass.	640		400	Pass.
α	—	0.988	Fit A	0	Pass.	0.924		0	Pass.

Table S1: The parameters of the OHC model and their values. Fit A and Fit B denote values found from comparison with experiment (Figs. 1C and 2C, respectively). Calc. and Scale indicate values calculated according to sections 1 and 8, respectively. Pass. refers to values for a passive hair bundle.

References

[1] Brownell WE (1983) Observations on a motile response in isolated outer hair cells. *Mechanisms of Hearing*, eds Webster WR, Aitken LM (Monash Univ. Press, Clayton), pp 5–10.

[2] Ó Maoiléidigh D, Jülicher F (2010) The interplay between active hair bundle motility and electromotility in the cochlea. *J. Acoust. Soc. Am.* 128:1175–1190.

[3] Martin P, Bozovic D, Choe Y, Hudspeth AJ (2003) Spontaneous oscillations by the hair bundles of the bullfrog's sacculus. *J. Neurosci.* 23:4533–4548.

[4] Martin P (2008) Active hair-bundle motility of the hair cells of vestibular and auditory organs. *Active Processes and Otoacoustic Emissions*, eds Manley GA, Fay RR, Popper AN (Springer, New York), pp 93–143.

[5] Bozovic D, Hudspeth AJ (2003) Hair-bundle movements elicited by transepithelial electrical stimulation of hair cells in the sacculus of the bullfrog. *Proc. Natl. Acad. Sci. USA* 100:958–963.

[6] Roongthumskul Y, Fredrickson-Hemsing L, Kao A, Bozovic D (2011) Multiple-timescale dynamics underlying spontaneous oscillations of saccular hair bundles. *Biophys. J.* 101:603–610.

[7] Kennedy HJ, Crawford AC, Fettiplace R (2005) Force generation by the mammalian hair bundle supports a role in cochlear amplification. *Nature* 433:880–883.

[8] Johnson SL, Beurg M, Marcotti W, Fettiplace R (2011) Prestin-driven cochlear amplification is not limited by the outer hair cell membrane time constant. *Neuron* 70:1143–1154.

[9] Tinevez J, Jülicher F, Martin P (2007) Unifying the various incarnations of active hair-bundle motility by the vertebrate hair cell. *Biophys. J.* 93:4053–4067.

[10] van Netten SM, Kros CJ (2000) Gating energies and forces of the mammalian hair cell transducer channel and related hair bundle mechanics. *Proc. R. Soc. Lond. B* 267:1915–1923.

[11] Beurg M, Nam JH, Crawford A, Fettiplace R (2008) The actions of calcium on hair bundle mechanics in mammalian cochlear hair cells. *Biophys. J.* 94:2639–2653.

[12] Ó Maoiléidigh D, Nicola EM, Hudspeth AJ (2012) The diverse effects of mechanical loading on active hair bundles. *Proc. Natl. Acad. Sci. USA* 109:1943–1948.

[13] Santos-Sacchi J (1992) On the frequency limit and phase of outer hair cell motility: effects of the membrane filter. *J. Neurosci.* 12:1906–1916.

[14] Hallworth R, Jensen-Smith H (2008) The morphological specializations and electromotility of the mammalian outer hair cell. *Active Processes and Otoacoustic Emissions*, eds Manley GA, Fay RR, Popper AN (Springer, New York), pp 145–189.

[15] Dannhof BJ, Roth B, Bruns V (1991) Length of hair cells as a measure of frequency representation in the mammalian inner ear? *Naturwissenschaften* 78:570–573.

[16] Dallos P (2003) Organ of Corti kinematics. *J. Assoc. Res. Otolaryngol.* 4:416–425.

[17] Ramamoorthy S, Nuttall AL (2012) Outer hair cell somatic electromotility in vivo and power transfer to the organ of corti. *Biophys. J.* 120:388–398.

[18] Lamb JS, Chadwick RS (2011) Dual traveling waves in an inner ear model with two degrees of freedom. *Phys. Rev. Lett.* 107:088101.

[19] Markin VS, Hudspeth AJ (1995) Modeling the active process of the cochlea: Phase relations, amplification, and spontaneous oscillation. *Biophys. J.* 69:138–147.

[20] Assad JA, Shepherd GMG, Corey DP (1991) Tip-link integrity and mechanical transduction in vertebrate hair cells. *Neuron* 7:985–994.

[21] Kozlov AS, Baumgart J, Risler T, Versteegh CPC, Hudspeth AJ (2011) Forces between clustered stereocilia minimize friction in the ear on a subnanometre scale. *Nature* 474:376–379.

[22] Dong X, Ospeck M, Iwasa KH (2002) Piezoelectric reciprocal relation of the membrane motor in the cochlear outer hair cell. *Biophys. J.* 82:1254–1259.

[23] Beurg M, Evans MG, Hackney CM, Fettiplace R (2006) A large-conductance calcium-selective mechanotransducer channel in mammalian cochlear hair cells. *J. Neurosci.* 26:10992–11000.

[24] Dallos P (1992) The active cochlea. *J. Neurosci.* 12:4575–4585.

[25] Richter CP, Emadi G, Getnick G, Quesnel A, Dallos P (2007) Tectorial membrane stiffness gradients. *Biophys. J.* 93:2265–2276.

[26] Emadi G, Richter CP, Dallos P (2004) Stiffness of the gerbil basilar membrane: Radial and longitudinal variations. *J. Neurophysiol.* 91:474–488.

[27] Edge RM, et al. (1998) Morphology of the unfixed cochlea. *Hear. Res.* 124:1–16.

[28] Reichenbach T, Hudspeth AJ (2010) A ratchet mechanism for amplification in low-frequency mammalian hearing. *Proc. Natl. Acad. Sci. USA* 107:4973–4978.

[29] Meaud, J.and Grosh K (2011) Coupling active hair bundle mechanics, fast adaptation, and somatic motility in a cochlear model. *Biophys. J.* 100:2576–2585.

[30] Preyer S, Renz R, Hemmert W, Zenner H, Gummer AW (1996) Receptor potential of outer hair cells isolated from base to apex of the adult guinea-pig cochlea: Implications for cochlear tuning mechanisms. *Aud. Neurosci.* 2:145–157.